Bio-clickable and Mussel Adhesive Peptide Mimics for Engineering Vascular Stent Surfaces

Zhilu Yang[1#], Xin Zhao[2#], Rui Hao[1], Qiufen Tu[1], Xiaohua Tian[3], Yu Xiao[1], Kaiqing Xiong[1], Miao Wang[3], Yonghai Feng[3], Nan Huang[1] & Guoqing Pan[3]**

[1]Key Laboratory of Advanced Technologies of Materials, Ministry of Education, School of Materials Science and Engineering, Southwest Jiaotong University, Chengdu, Sichuan 610031, China.

[2]Department of Biomedical Engineering, the Hong Kong Polytechnic University, Hung Hom, Hong Kong, China.

[3]Institute for Advanced Materials, School of Materials Science and Engineering, Jiangsu University, Zhenjiang, Jiangsu 212013, China.

co-first author

To whom correspondence may be addressed.

*** E-mail**: huangnan1956@163.com (N.H.); panguoqing@ujs.edu.cn (G.P.)

Competing Interest Statement: The authors declare no competing interests.

Author Contributions. Z.Y. and X.Z. contributed equally to this work; Z.Y., X.Z., N.H. and G. P. designed research; Z.Y., X.Z., R.H., Q.T., X.T., Y.X., K.X., M.W. and Y.F. performed research; Z.Y., X.Z., R.H., Q.T., X.T. and Y.X. analyzed data; Z.Y., X.Z., N.H. and G. P. wrote the paper.

This file includes:

Main Text

Scheme 1; Figures 1 to 7

Word Count: 5244 (without references)

Reference Count: 54

Abstract: Thrombogenic reaction, aggressive smooth muscle cell (SMC) proliferation and sluggish endothelial cell (EC) migration onto bio-inert metal vascular stents make post-stenting re-endothelialization a dilemma. Here, we report an easy to perform, biomimetic surface engineering strategy for multiple functionalization of metal vascular stents. We first design and graft a clickable mussel-inspired peptide onto the stent surface via mussel-inspired adhesion (Figure 1). Then, two vasoactive moieties (i.e., the nitric oxide (NO)-generating organoselenium (SeCA) and the endothelial progenitor cell (EPC)-targeting peptide (TPS)) are clicked onto the grafted surfaces via bio-orthogonal conjugation. We optimize the blood and vascular cell compatibilities of the grafted surfaces through changing the SeCA/TPS feeding ratios. At the optimal ratio of 2:2, the surface-engineered stents demonstrate superior inhibition of thrombosis and SMC migration and proliferation, promotion of EPC recruitment, adhesion and proliferation, as well as prevention of in-stent restenosis (ISR). Overall, our biomimetic surface engineering strategy represents a promising solution to address clinical complications of cardiovascular stents and other blood-contacting metal materials.

Significance: An ideal metal vascular stent has multiple properties for successful re-endothelialization. These properties include (1) inhibiting thrombosis by preventing platelet activation/adhesion, (2) suppressing smooth muscle cell (SMC) migration/proliferation, and (3) accelerating endothelial cell (EC) migration/proliferation. With an easy-to-perform, two-step surface bioengineering approach, the multi-functionalized stents reported here contain two vasoactive moieties (i.e., the nitric oxide (NO)-generating organoselenium (SeCA) and the endothelial progenitor cell (EPC)-targeting peptide (TPS)) to satisfy all requirements. The surface engineering strategy presented here can be translated into new clinical coatings for cardiovascular stents and will benefit enormously and globally the cardiovascular disease patients; it will, moreover, offer insights to engineering surfaces of blood-contacting devices.

Since the first vascular endoprosthesis developed for relieving arterial obstruction in 1987,[1] vascular stent implantation has become the central therapy to treat cardiovascular diseases in clinics.[2] The popularity of stenting is owing to the immediate effects of considerably reducing acute vessel closure. However, the long-term clinical success of stenting is limited due to complications such as in-stent restenosis (ISR, i.e., thrombosis and intimal hyperplasia at the interfaces of vascular implants).[3, 4, 5, 6, 7, 8] ISR occurs when endothelium is damaged by stenting, which provokes pro-thrombogenic reactions, triggers platelet adhesion, aggregation and activation on the metal stents, and narrows the stented coronary artery considerably. This may eventually result in failure of vascular stents, and other complications including sudden death or non-fatal myocardial infarction.[9, 10] The damages of endothelium will also trigger excessive smooth muscle cell (SMC) migration from vascular middle membrane and proliferation at the lesion (i.e., intimal hyperplasia). Accompanied by extracellular matrix (ECM) deposition, such events lead to eventually ISR.[11, 12] Hence, platelet and SMC suppression are essential for combatting ISR.

Earlier strategies for ISR prevention rarely considered endothelial regeneration. For instance, drug-eluting stents (DESs) are effective in reducing early thrombosis and inflammation, as well as inhibiting SMC migration and proliferation. However, the delayed vascular and especially endothelial healing usually result in high risk of late stent thrombosis (LST) and ISR.[13] Later, another strategy, known as *in vitro* endothelialization, was developed by pre-seeding endothelial cells (ECs) onto vascular device surfaces prior to implantation.[14] Nevertheless, the resulting endothelium shows detachment due to the mechanical interactions during stenting and degenerative performance trigged by aggregation of the detached cells.

In contrast, surface bioengineering approaches have shown inherent superiority as they endow the vascular implants with rapid restoration of functional endothelium after implantation *in vivo* (i.e., *in situ* endothelialization).[15, 16, 17, 18, 19] By incorporating endothelium-specific motifs, vascular implant surfaces can be tailored with desired properties conducive to *in situ* endothelialization, such as capturing endothelial progenitor cells (EPCs) from the surrounding environment,[20, 21, 22, 23, 24] and releasing vasoactive mediators to mimic endothelial functions and microenvironments.[25, 26] Long-term effects of these endothelium-specific surface engineering strategies are, however, far from ideal due to the complexity of endothelium functions and the monotonicity of surface bioactivity on these vascular implants. In addition, current surface bioengineering strategies mainly rely on chemical conjugation of bioactive molecules; this biomolecule grafting approach will inevitably consume the active groups (e.g., NH_2, SH) of a biomolecule, potentially sacrificing its bioactivity.[27, 28] Moreover, these methods mostly involve

tedious chemical reactions and sophisticated surface treatments. Apart from potential damage to bioactivity, the complexity of traditional chemical reactions also compromises the controllability, operability and reproducibility of a multicomponent bioactive surface.

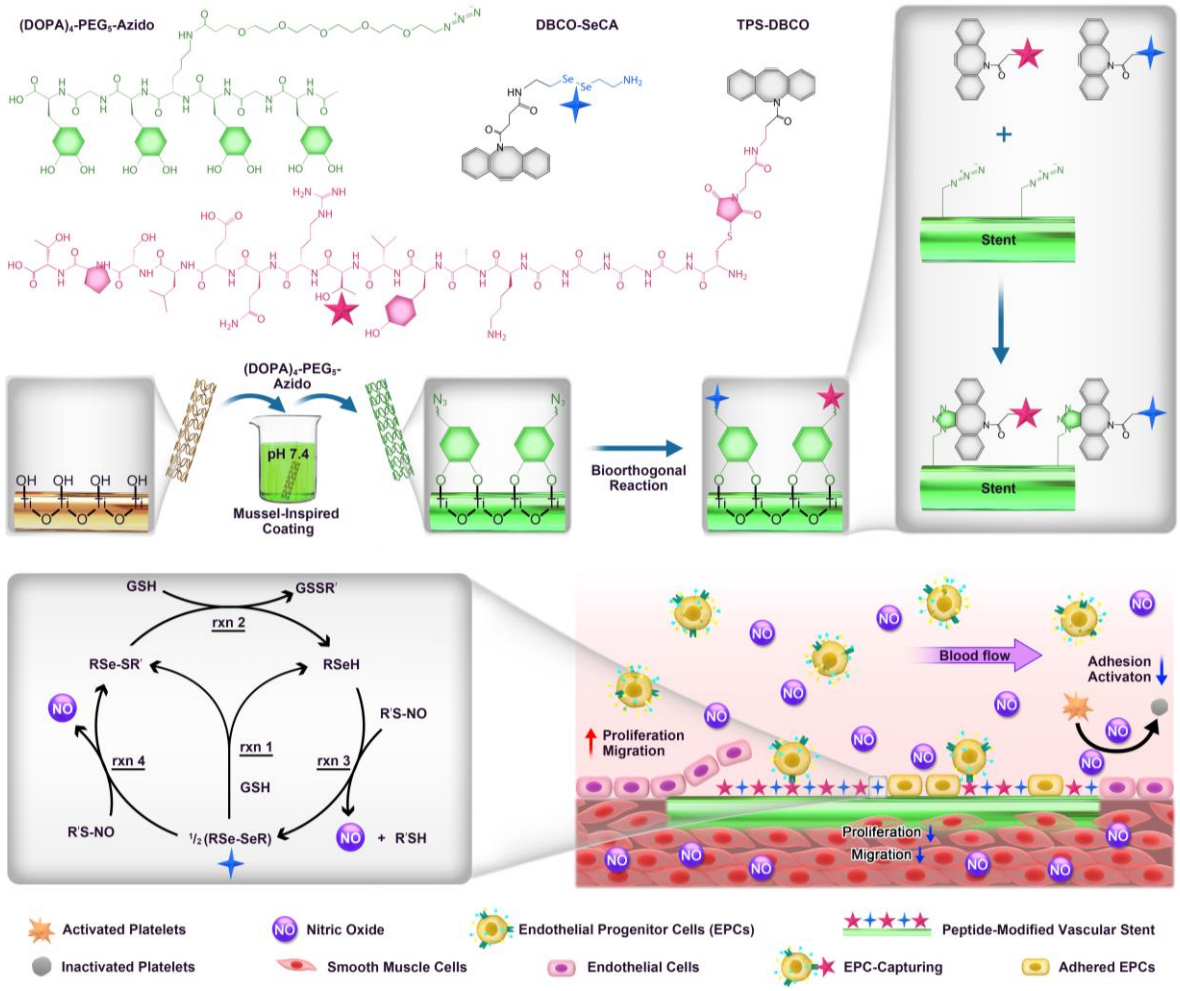

Scheme 1. a) Structural formula of the clickable mussel-inspired peptide ($(DOPA)_4$-PEG_5-Azide), NO-generating organoselenium (DBCO-SeCA) and EPC-binding peptide (TPS-DBCO). b) Surface co-grafting on representative vascular stents through mussel-inspired coordinative interactions and bio-orthogonal click chemistry. c) The catalytic reactions of NO-generation process by SeCA and the proposed mechanism of SeCA/TPS co-grafted stents for anti-platelet adhesion, SMC inhibition, EPC-homing, EC growth and re-endothelialization.

Here, we functionalize metal vascular stents in a two-step manner by combining mussel-inspired molecular adhesion and bio-orthogonal click chemistry (**Scheme 1**). First, we coat the stent surfaces with a clickable mussel-inspired peptide with azido (N_3) and catechol groups by mimicking the molecular structure of mussel foot proteins (Mfps).[29, 30] Similar to Mfp adhesion, the mussel-inspired peptide can stably bind onto the metal stents via spontaneous metal-catechol coordination. Afterwards, two vasoactive moieties, organoselenium (a glutathione peroxidase (GPX)-like catalyst capable of decomposing endogenous S-nitrosothiols (RSNOs) into nitric oxide (NO)) [31] and EPC-binding TPS peptide (a human blood outgrowth endothelial cell

(HBOEC)-specific peptide for EPC targeting),[32, 33] are modified with N_3-complementary reactive group dibenzylcyclooctyne (DBCO).[34] The surface-bound N_3 groups then enable grafting of DBCO-modified active moieties through bio-orthogonal N_3-DBCO click reaction. Due to the specificity, rapidness and thoroughness of bio-orthogonal chemistry,[34] vascular stents with tunable dual functions (i.e., NO-generating and EPC-capturing properties) can be readily obtained via a feeding-dependent co-grafting process. The motivation to use NO-generating compound comes from the anti-platelet aggregation and SMC inhibition capabilities of NO molecules,[35, 36,37] and the TPS peptide due to its homing capabilities of circulating blood EPCs, thus accelerating the endothelialization process. To the best of our knowledge, this is the first study to integrate NO-generating and EPC-capturing moieties into one cardiovascular stent coating system while involving only simple, specific, rapid and reproducible procedures. This allows for easy mass fabrication and popularization of our cardiovascular coatings. We discover that the SeCA-catalyzed NO generation and TPS-induced EPC capture have contributed synergistically and successfully to *in vitro* anti-thrombosis, SMC inhibition and endothelial cell (EC) promotion. At the optimal SeCA/TPS feeding ratio of 2:2, we observe excellent *in vivo* endothelialization and ISR prevention. We expect our strategy to provide a facile approach for rational bioengineering of vascular stents with optimal multi-functions. Such vascular stents can tackle the complicated endothelial pathological microenvironments, promote rapid re-endothelialization, and ultimately improve clinical outcomes of stenting by reducing the restenosis.

Results

Molecular synthesis and surface functionalization. The clickable mussel-inspired peptide was prepared by solid-phase peptide synthesis according to our previously reported method.[38, 39, 40] Briefly, 3,4-dihydroxy-L-phenylalanine (DOPA), a catecholic amino acid abundant in Mfps,[30, 41] was introduced into the peptide sequence using acetonide-protected Fmoc-DOPA(acetone)-OH. To facilitate the mussel-like molecular adhesion onto the metal substrates and leave accessible clickable groups for second-step click reaction, tetravalent DOPA with one amino acid interval and polyethylene glycol (PEG)-linked azide were integrated to obtain a clickable mussel-inspired adhesive peptide Ac-(DOPA)-Gly-(DOPA)-(Lys-PEG_5-Azide)-(DOPA)-Gly-(DOPA)-COOH (i.e., $(DOPA)_4$-PEG_5-Azide) (**Scheme 1a**). As two key vasoactive factors for endothelium regeneration, the NO-generating organoselenium (C, SeCA)[31, 42] and EPC-binding TPS peptide (Thr-Pro-Ser-Leu-Glu-Gln-Arg-Thr-Val-Tyr-Ala-Lys) were conjugated with DBCO via *N*-hydroxysuccinimide-amine and maleimide-thiol coupling, respectively (**Scheme**

1a). The obtained DBCO-capped NO-catalyst (DBCO-SeCA) and EPC-binding peptide (TPS-DBCO) thus could be easily connected with $(DOPA)_4$-PEG_5-Azide-bound surfaces, which would enable a flexible biofunctionalization (**Scheme 1b**). After purification through high-performance liquid chromatography (HPLC), the three synthesized molecules were then characterized with electrospray ionization mass spectrometry (ESI-MS). The monoisotopic mass $[M+H]^+$ of $(DOPA)_4$-PEG_5-Azide, $[M-H]^-$ of DBCO-SeCA, and $[M+2H]^{2+}$ of TPS-DBCO were measured at 1336.8, 534.1 and 1077.0 Da, corresponding to their theoretical molecular weight 1335.6, 535.0 and 2152.0 respectively (**Figure 1a-c**). These results demonstrated the successful synthesis of azide-modified mussel adhesive peptide mimic and DBCO-capped endothelial growth factors.

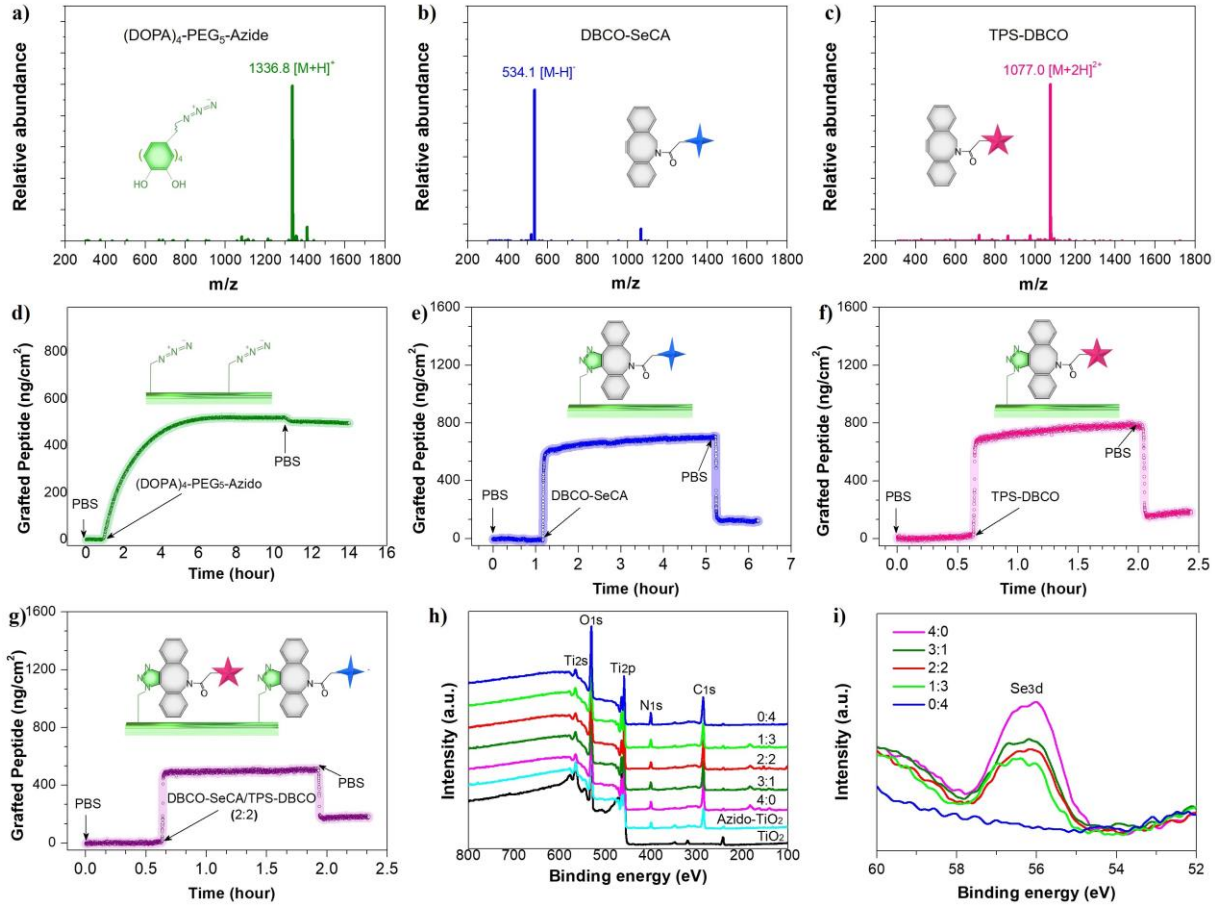

Figure 1. ESI mass spectrum of a) $(DOPA)_4$-PEG_5-Azide, b) DBCO-SeCA and c) TPS-DBCO. d) Real-time monitoring of the binding of $(DOPA)_4$-PEG_5-Azide on a TiO_2-coated chip determined by QCM. e) DBCO-SeCA, f) TPS-DBCO and g) DBCO-SeCA/TPS-DBCO co-grafting process on the $(DOPA)_4$-PEG_5-Azide-bound chips. h) XPS full spectrum and i) Se3d signal peaks of the grafted surfaces.

Multivalent catechol-containing molecules could easily and stably bind onto the metal oxide surfaces through coordination. In this study, we modified the TiO_2-coated 316L stainless steel (SS) with $(DOPA)_4$-PEG_5-Azide. The $(DOPA)_4$-PEG_5-Azide can be strongly chelated to

the TiO_2 coated surfaces based on the catecholato-Ti coordinate covalent bond. We used TiO_2 coated 316 L SS (noted as TiO_2 in this study) as a control as TiO_2 coated stents (e.g., HELIOS^{TM}) are widely used clinically,[43] and they have demonstrated improved hemocompatibility, cytocompatibility and histocompatibility compared to conventional naked 316L SS stents.[44] To monitor the peptide binding and biomolecular grafting, we used quartz crystal microbalance (QCM). As shown in **Figure 1d**, $(DOPA)_4$-PEG_5-Azide demonstrated steady binding onto the QCM chips and reached up to a maximal binding capacity of 498 ng·cm^{-2} (i.e., 372 pmol·cm^{-2}), indicating the high-efficiency and spontaneous adhesion onto TiO_2-coated surfaces. Note that the binding capacity here is higher than that of our previous work (274 pmol·cm^{-2}),[38] probably due to the improved catechol orientation for surface binding. Then, the azide-modified chips (TiO_2-Azide) were incubated with DBCO-SeCA or TPS-DBCO for bio-orthogonal conjugation (**Figures 1e** and **f**). According to Quartz Crystal Microbalance with Dissipation monitoring (QCM-D) analysis, the grafting processes started in a few minutes, and the maximal grafting amount for DBCO-SeCA and TPS-DBCO were 119 and 181 ng·cm^{-2} (224 and 84 pmol·cm^{-2}), respectively. Because of steric hindrance, not all of the azido groups could be grafted with DBCO-capped molecules, and larger molecules (e.g., TPS-DBCO) resulted in less grafting. Further study on dual-functionalization was also performed using a mixture of DBCO-SeCA and TPS-DBCO (2:2 in molar ratio), and the co-grafting amount showed a median value around 169 ng·cm^{-2} (**Figure 1g**). Surface elemental compositions with different feeding molar ratios of DBCO-SeCA and TPS-DBCO (i.e., 4:0, 3:1, 2:2, 1:3 and 0:4) were then characterized by X-ray photoelectron spectrum (XPS). As shown in **Figure 1h**, a gradual enhancement in N 1s signal at 400.12 eV was found on the co-grafted surfaces with increasing proportion of TPS-DBCO. Likewise, the Se 3d signal weakened as the feeding ratio of DBCO-SeCA decreased (**Figure 1i**). This result indicated that the bio-orthogonal conjugation of a grafted moiety depends on its feeding amount, allowing for optimization and control of surface bioactivities.

***In vitro* NO generation and EPC capture.** For *in vitro* experiments, we used the commercially available TiO_2-coated 316L stainless steel (SS) foil as the material is widely used for vascular stent. NO release was first determined by a real-time chemiluminescent assay.[45] Phosphate buffer saline (PBS) solution (pH 7.4) containing 10 μM L-glutathione (GSH, an endogenous reductant for selenol (SeH) generation) and 10 μM *S*-nitrosoglutathione (GSNO, an endogenous NO donor for SeH-catalyzed NO generation) was used to simulate the blood environment. Real-time monitoring of NO flux revealed a SeCA dose-dependent NO generation (**Figure 2a**). With the decreased proportion of DBCO-SeCA for surface grafting, NO generation slowed down. This

result indicated the feasibility of bio-orthogonal co-grafting method for not only efficient SeCA conjugation but also controllable NO-generation.

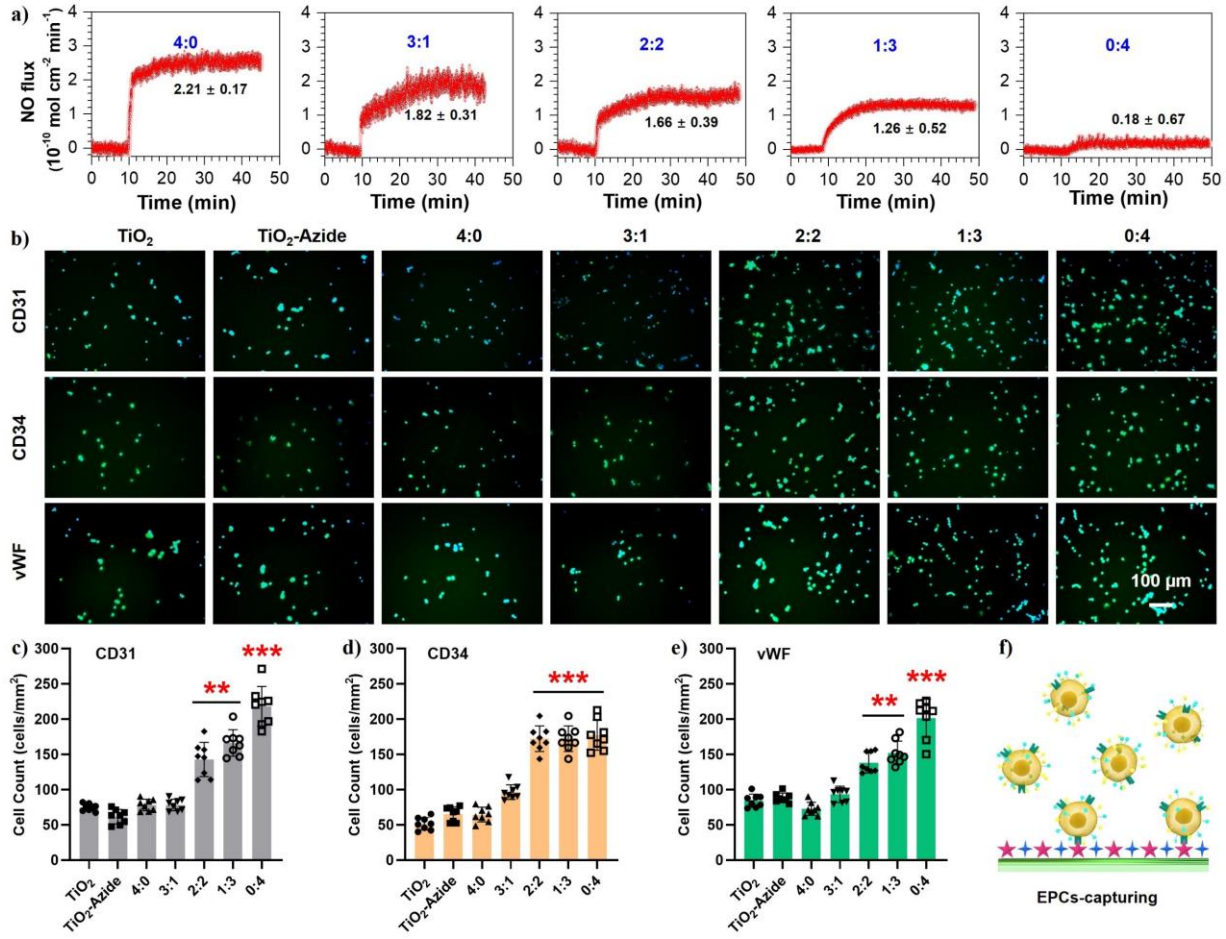

Figure 2. Effects of SeCA/TPS feeding ratio on NO generation (a), EPC capture (b-e), and EPC capture mechanism (j). a) Rate of NO generation decreased as the SeCA/TPS feeding ratio decreased, indicating a SeCA dose-dependent fashion. b) Endothelial cell markers had higher expressions as the proportion of TPS in the SeCA/TPS increased, demonstrating the EPC-homing abilities of TPS peptide. Quantitative analyses further confirmed the higher adhesion of endothelial cells on the stents by immunostaining of c) CD31, d) CD34, and e) vWF. f) EPCs are captured on the modified stent surface via molecular recognition of TPS peptides.

Another endothelium-related bioactivity is the EPC specificity of TPS peptide. Peripheral blood cultures contain a number of HBOECs, which are a population of late-EPCs with endothelial phenotype, high proliferative capacity, and several EC markers, such as CD31, CD34 and von Willebrand factor (vWF).[46] TPS peptide-grafted surfaces in blood environment can induce EPC recognition, adhesion and proliferation, which would facilitate re-endothelialization on vascular stents. To determine the EPC-targeting activity, mesenchymal stem cells (MSCs) were isolated from Danforth's short tail (Sd) mouse for endothelial differentiation into EPCs (**Figure S1**). The untreated 316L SS substrates (i.e., TiO_2 group) and $(DOPA)_4$-PEG_5-Azide-treated substrates (TiO_2-Azide group) were used as controls. All substrates were placed in a

chamber with a flow of EPC suspension for 2 h (**Figure S2**), and the captured cells on different surfaces were stained by immunofluorescence for CD31, CD34, and vWF. As shown in **Figure 2b**, all the groups could elicit recognizable EPC adhesion, and the co-grafted groups with higher TPS-DBCO feeding (e.g., 2:2, 1:3 and 0:4) displayed evidently stronger EPC-capturing activity compared to the others. Quantitative analysis further confirmed this finding (**Figure 2c-e**). Furthermore, the results also indicated that significantly enhanced EPC capture could only be observed when the TPS-DBCO feeding ratio was higher than 50%.

***In vitro* anti-platelet adhesion and *ex vivo* anti-thrombogenic properties.** At the early stage after implantation, thrombosis on stents is a crucial problem. As a star gaseous signaling molecule, endogenous NO affects a number of cellular processes. In the cardiovascular system, NO can bind to the heme moiety of soluble guanylate cyclase (sGC), leading to sGC activation and subsequent cyclic guanosine monophosphate (cGMP) upregulation.[36, 47] The resultant NO-cGMP signaling and a series of cascades modulate numerous key physiological processes including the prevention of platelet activation and aggregation, inhibition of SMC proliferation, and promotion of EC growth.[48] Hence, surface engineering of metal stents with NO-generating property is a bioinspired solution to promote endothelization and to reduce ISR. Here, we first investigated platelet adhesion on the co-grafted 316L SS substrates. For all *in vitro* experiments, extra NO donor (GSNO, 10 μM) was used to level the concentrations of RSNOs in physiology. Without donor supply, all groups had substantial platelet adhesion and activation in 30 min, and the grafted groups showed almost no inhibition in the amount and activation rates of adhered platelets (**Figure S3**). Upon adding donor to generate NO, significant changes were observed in the SeCA-containing groups. As shown in **Figure 3a**, the control groups (TiO_2 and TiO_2-Azide) and the grafted group without SeCA (0:4) still had evident platelet adhesion, and the spread morphology of platelets showed a high degree of activation and aggregation. In contrast, the SeCA-containing groups (4:0, 3:1, 2:2 and 1:3) all showed substantially reduced platelet adhesion with inactive spherical state. Quantitative analysis revealed that only the grafted groups with higher DBCO-SeCA feeding ratios (4:0, 3:1 and 2:2) could significantly inhibit platelet adhesion and activation (**Figure 3b** and **c**). Moreover, the inhibitory efficiency showed a DBCO-SeCA feeding-dependent manner, indicating the importance of sufficient SeCA content for platelet inhibition.

We further investigated the anti-thrombogenic property of our stents using *ex vivo* perfusion experiments.[49] The 316L SS foils with different surface components were curled up and placed onto the inner walls of commercially available cardiopulmonary perfusion tubes, which were

then connected to a rabbit arteriovenous (AV) shunt (**Figure 3d**). The ability of the grafted surfaces to support blood flow was evaluated in the presence of NO donor. After 2 h of circulation, the sizes of occlusive thrombosis, thrombus weight, and blood flow rates in the circuit were evaluated (**Figure 3e-h**). We found that there was serious thrombus formation on the three SeCA-free control groups (i.e., TiO_2, TiO_2-Azide and 0:4). On the other hand, only a small number of cruor were observed on the groups with high SeCA contents (i.e., 4:0, 3:1 and 2:2) **(Figure 3f).** Quantitative analysis further confirmed the above results and demonstrated significant reduction in thrombosis formation of the SeCA grafted groups with mean thrombosis weight (**Figure 3f**, 4.26 mg vs 9.40 mg), blood flow rate (**Figure 3g**, 86.34% vs 36.43%) and occlusion percentage(**Figure 3h**, 14.73% vs 61.03%) compared to the SeCA-free controls. The above results have suggested the significance of sufficient SeCA content for efficient anti-thrombosis.

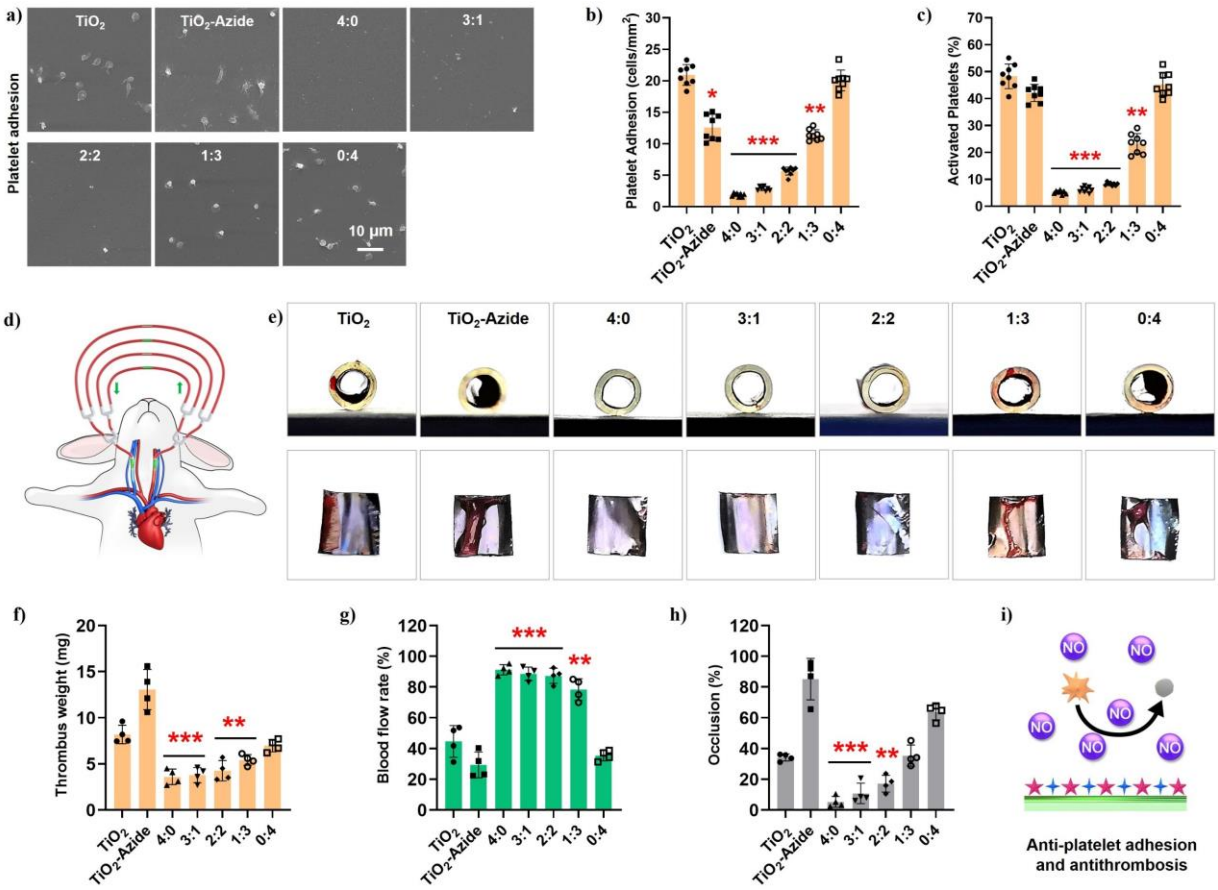

Figure 3. a) SEM images, b) average density, and c) activation rates of the adhered platelets after incubation with different 316L SS substrates supplemented with NO donor. d) Schematic illustration of the rabbit AV shunt model. e) Cross-sectional photographs of tubing and the corresponding thrombus formed in different groups. Quantitative results of f) the thrombus weight, g) blood flow and h) occlusion rate in different groups. i) Schematic antiplatelet adhesion and activation on the co-grafted surface. Statistically significant differences are indicated by $*p < 0.05$, $**p < 0.005$, $***p < 0.001$ compared with the bare surface (the TiO_2 group).

***In vitro* vascular cell growth.** In addition to antiplatelet and antithrombotic properties, we also explored the effect of co-grafted surfaces on SMC inhibition because of its correlation to neo-intimal hyperplasia. Human umbilical arterial smooth muscle cells (HUASMCs) (**Figure S4**) were seeded onto different 316L SS substrates, and the morphology, amount and proliferation of adhered HUASMCs were characterized by fluorescence staining, counting and cholecystokinin octapeptide (CCK-8) assay, respectively (**Figures 4a** and **b**, **S5**). The adhesion and growth of HUASMCs on the SeCA-free groups (TiO_2, TiO_2-Azide and 0:4) showed no significant difference regardless of whether the medium was supplemented with donor. In contrast, the SeCA-containing groups (4:0, 3:1, 2:2 and 1:3) could efficiently inhibit HUASMC adhesion and proliferation when the medium was supplemented with donor. The result further indicated that, to generate sufficient NO for platelet and SMC inhibition, the feeding ratio of SeCA-DBCO in co-grafting process should be no less than 50%.

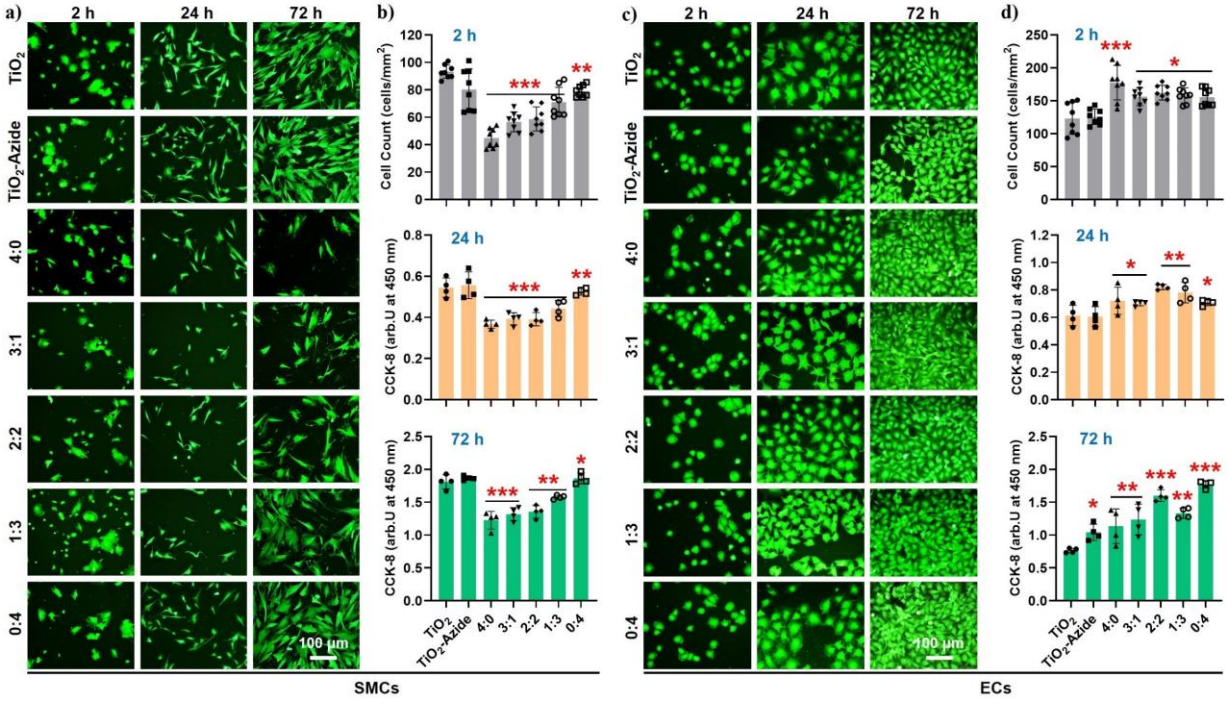

Figure 4. a) and b) HUASMC adhesion and proliferation in medium supplemented with NO donor. c) and d) HUVEC adhesion and proliferation with NO donor supplement. Statistically significant differences are indicated by $*p < 0.05$, $**p < 0.005$ or $***p < 0.001$ compared with the control group.

Efficient EC proliferation and migration are another key process to generate endothelium on the implanted stents. Since NO molecule and TPS peptide both could provide EC-friendly microenvironment, human umbilical vein endothelial cells (HUVECs) **(Figure S4)** were then used to investigate EC-compatibility of the grafted substrates (**Figure 4c** and **d**). In this study, HUVECs are used instead of human aortic endothelial cells (HAECs) due to their ready availability and similar cellular characteristics to HAECs in a two-dimensional culture.[42, 50, 51, 52]

We found that, with donor supplement, all grafted groups showed significant enhancement of HUVEC adhesion and proliferation compared with the ungrafted controls. Without donor supplement, such enhancement all experienced a certain decrease but still showed significant differences (**Figure S6**). These results demonstrated that NO production by SeCA and the EC-TPS binding synergistically promote EC attachment, spreading and proliferation. Together, our stents showed desirable properties for vascular endothelialization (i.e., the enhancement of EC migration but opposite effects on SMCs).

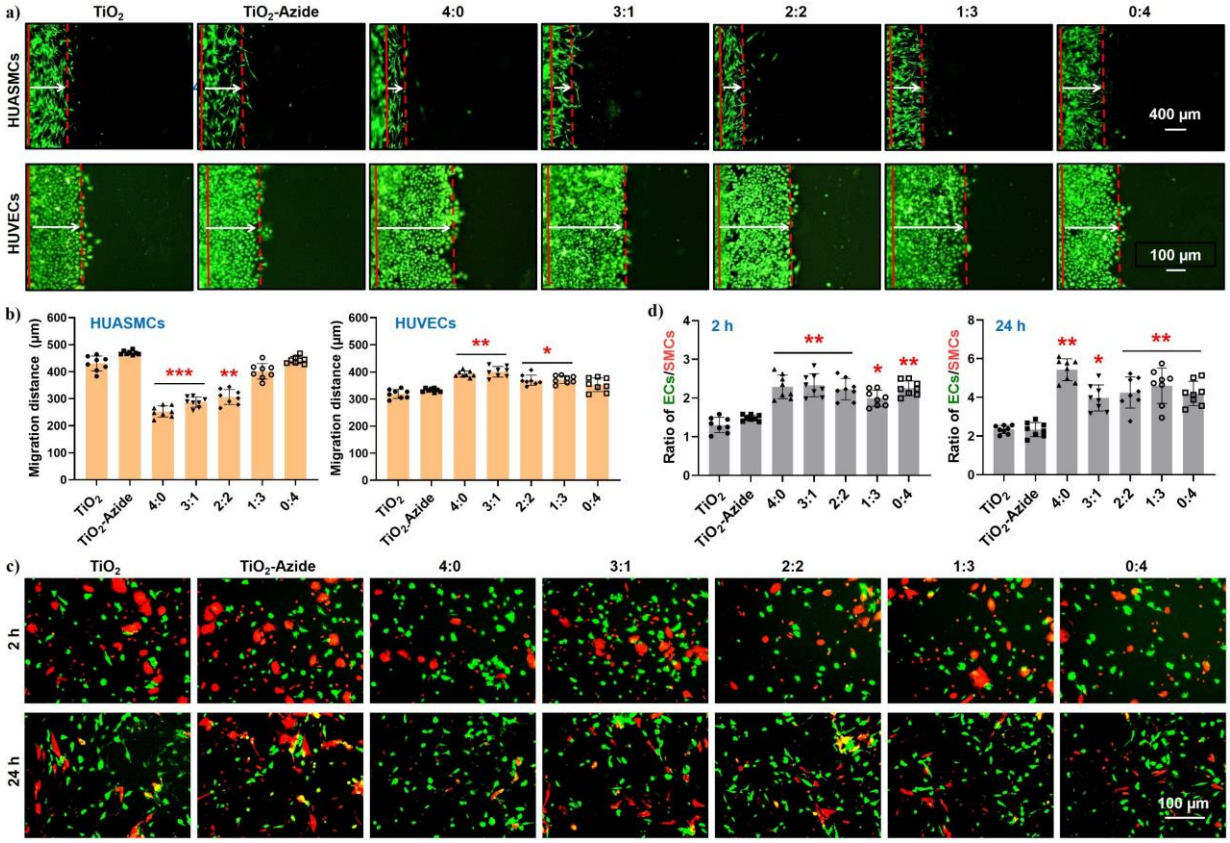

Figure 5. a) and b) Migration of HUVECs and HUASMCs on different 316L SS surfaces after 1 day of culture with donor supplement. c) and d) Competitive growth of HUVECs (green) and HUASMCs (red) on different surfaces with donor supplement. Statistically significant differences are indicated by $*p < 0.05$, $**p < 0.005$ or $***p < 0.001$ compared with the control group.

To confirm this deduction, the migration of these two vascular cells were evaluated and compared. The competitive growth behaviors between HUVECs and HUASMCs on different samples was conducted to deduce the *in vivo* re-endothelialization efficacy of our coatings. We found that in the absence of NO donor, migrations of HUVECs and HUASMCs on all surfaces showed no significant difference (**Figure S7**). Upon the addition of donor, cell migration on the NO-generating surfaces (e.g., 4:0, 3:1 and 2:2) changed remarkably (**Figure 5a** and **b**). Taking the group of 2:2 for example, cell migration distance showed a decrease of 30.8% for HUASMCs but an increase of 15.0% for HUVECs. Cell migration on the TPS mono-grafted group (i.e., 0:4)

showed no changes regardless of donor supplement. These results jointly demonstrated that NO produced by SeCA could provide EC-friendly microenvironment to enhance EC motility and inhibit excessive SMC growth. Such feature is also expected to bring in rapid regeneration of endothelium and reduced neo-intimal proliferation after vascular stent implantation. However, the ECs compete with SMCs *in vivo*, in particular, after vascular injury or stenting. To investigate the selectivity of these grafted surfaces for vascular cell growth, co-culture (1:1) of HUVECs (green staining) and HUASMCs (red staining) was carried out. As shown in **Figure S8**, without donor supplement in culture medium, the co-grafted groups with high DBCO-TPS feeding ratios could elicit enhanced EC adhesion in the first 2 h, whereas no significant difference was found in all groups after 24 h. This finding, together with the negligible effect of TPS peptide on EC migration, indicated that TPS could only enhance the early EC recognition and adhesion but was irrelevant to the following EC proliferation and migration. After the addition of donor, EC adhesion and proliferation on all the grafted groups exhibited an overwhelming enhancement against those of SMCs (**Figure 5c** and **d**). For example, the ratios of HUVECs to HUASMCs adhered onto the grafted 316L SS substrates all showed a nearly 2-fold increase than those of the controls, demonstrating their excellent selectivity for EC growth. This beneficial effect on ECs (enhancement) and SMCs (inhibition) may be due to the activation of cGMP expression in the NO-cGMP cell signaling pathway and the selective apoptosis of SMCs.[53] The above results justified the feasibility of our strategy to inhibit SMC-caused intimal hyperplasia and to generate a pure *in situ* endothelium onto an optimized co-grafted stent surface *in vivo*.

On the whole, the above experiments indicated that the grafted amounts of SeCA and TPS depend on their ratio during bio-orthogonal grafting, and both molecules are blood- and vascular cell-compatible. On one hand, increased NO generation results in lower thrombosis, attenuated SMC inhibition and enhanced EC growth. On the other hand, the increase of EPC-binding peptide on the surfaces facilitates EPC-homing and EC growth. To rationally select an optimal co-grafting condition for vascular stents, all the *in vitro* and *ex vivo* results were summarized in a heat map by normalizing the desired properties of a vascular stent (**Figure 6a**). The grafted groups with significant differences compared to the control (i.e., the TiO_2 group) were also marked with stars. As clearly shown in the heat map, the co-grafted surfaces with SeCA/TPS feeding ratio at 2:2 are the most superior, with efficient anti-thrombosis and SMC inhibition, and excellent EPC-binding, EC adhesion and proliferation. Therefore, this optimized grafting condition was used for subsequent assessment of *in vivo* efficacy of *in situ* endothelialization and prevention of restenosis.

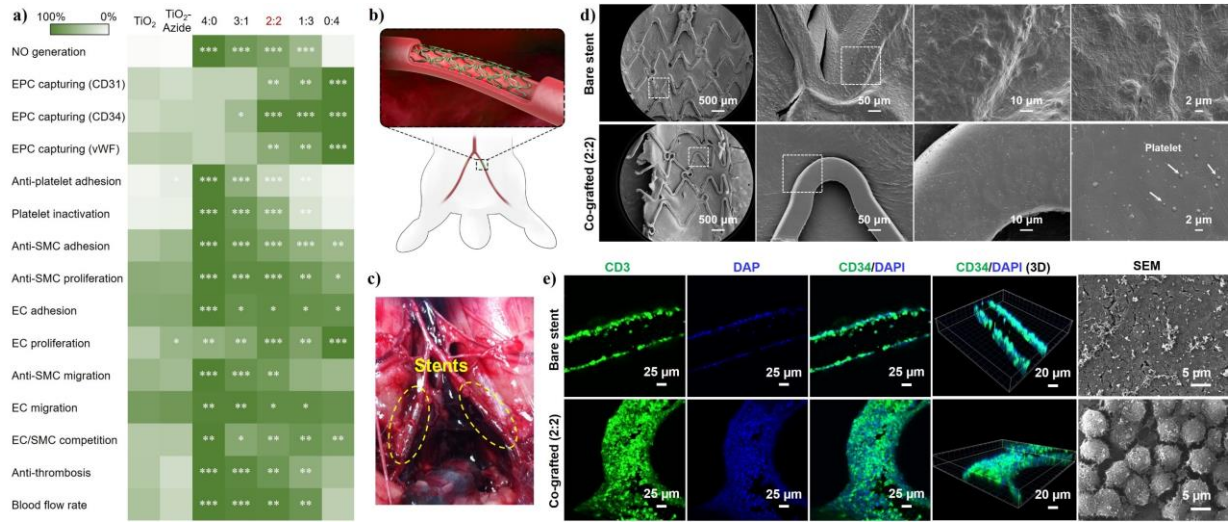

Figure 6. a) The heat map of vascular-stent-preferred properties. Statistically significant differences are indicated as $*p < 0.05$, $**p < 0.005$, $***p < 0.001$ compared with the control stents. b) Schematic of stent implantation in the iliac arteries of rabbits. c) Experimental photographs of the implanted stents using New Zealand white rabbits. d) Platelet adhesion and e) EPC binding onto the harvested stents after 2 h of implantation.

***In vivo* anti-coagulation and EPC capture**. The ungrafted (control) and co-grafted (2:2) 316L SS vascular stents were both implanted into the iliac arteries of New Zealand white rabbits with the aid of angiography (**Figure 6b** and **c**). Short-term stent implantation (2 h) was first carried out to evaluate blood clotting and EPC capture. As shown in the SEM images (**Figure 6d)**, the control stent surface was covered with a layer of activated platelets and fibrin. In contrast, there was only a small number of scattered and inactivated platelets with spherical shapes on the co-grafted stent. The result was consistent with those of *in vitro* anti-platelet adhesion and *ex vivo* anti-thrombosis experiments, confirming the early anti-coagulant property of the SeCA/TPS co-grafted stents.

To investigate the practical efficacy for early EPC homing, we further assessed the *in vivo* EPC capture capacity. The rabbits were injected with granulocyte colony-stimulating factor (G-CSF) to mobilize EPCs into the blood in advance. 2 h after implantation, the stents were harvested and immunostained for CD31, an EC marker highly expressed at endothelial cell-cell junctions (**Figure 6e**).[54] As expected, the surface of co-grafted stents showed full green fluorescence, indicating the excellent EPC capture in the first 2 h. On the other hand, the control stent surface showed only non-specific binding of EPCs, and could not form a confluent cell layer. Similar results with detailed information were also observed in the SEM images of the harvested stents, in which close-arranged EPCs could be found only on the co-grafted stents. Undoubtedly, the co-grafted stents showed potent EPC capture capacity for early EPC

recruitment, which would facilitate rapid re-endothelialization and reduce later neo-intimal hyperplasia.

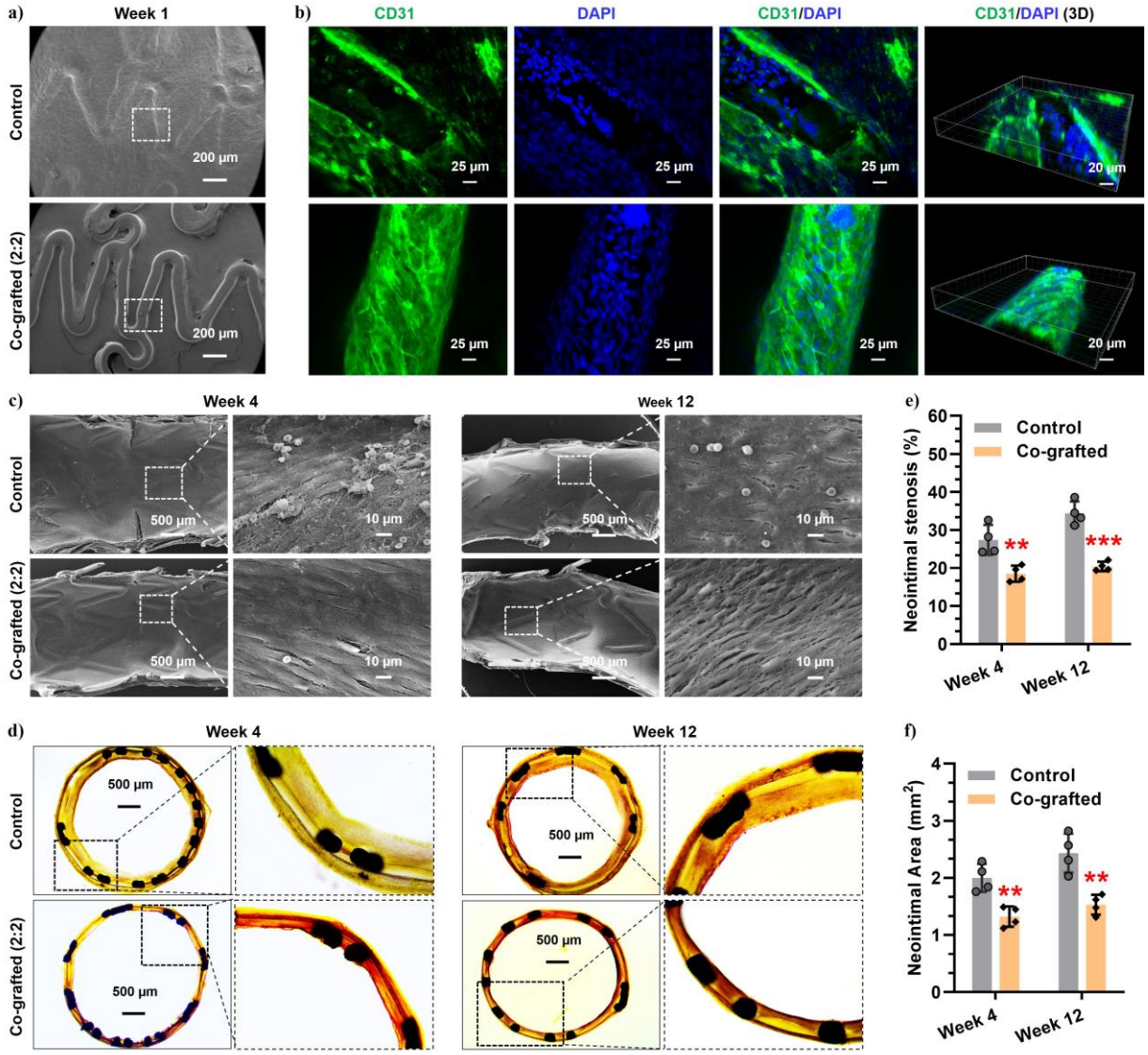

Figure 7. Long-term stent implantation *in vivo*. a), b) and c) Re-endothelialization on the control and co-grafted stents after implantation for 1, 4 and 12 weeks. d), e) and f) Histomorphometric and quantitative analysis of ISR prevention *in vivo*. Statistically significant differences are indicated by $^{**}p < 0.005$, $^{***}p < 0.001$ compared with the control stents.

***In vivo* re-endothelialization and anti-restenosis.** Long-term implantation was further performed to demonstrate the potential of the co-grafted stents for re-endothelialization and prevention of ISR. All the *in vivo* experiments were carried out with early granulocyte colony-stimulating factor (G-CSF) injection for EPC mobilization but without donor supplement. Stented iliac arteries with implanted stents were harvested after 1, 4 and 12 weeks of stent deployment. SEM images showed that, in the first week, the surface of control stent was fully covered by a thick layer of matrix, whereas the co-grafted stents still showed clear outline (**Figure 7a**). Immunostaining revealed that the co-grafted stents were well-adhered with an intact

layer of ECs, but the heavily covered layer on the control stents was partly composed of ECs located just onto the edge of stent skeleton, probably due to the migration of ECs from the surrounding endothelial tissue (**Figure 7b**). This finding further indicated the excellent and sustained EPC-homing property for early endothelialization *in vivo*. Given this, the interfacial re-endothelialization after 4 and 12 weeks of stent implantation was further evaluated. As shown in **Figure 7c**, although the control stent surface was covered by a layer of cells in weeks 4 and 12, most of the cells were inconsistent with endothelial morphology. Excitingly, the co-grafted vascular stent was fully covered by an intact EC monolayer, which elongated and aligned to the blood flow direction under sheared condition. These findings verified that the dual-functional surface with optimized NO generation and EPC capture could significantly promote re-endothelialization process on vascular stents.

Histomorphometric analysis was finally performed to examine the effects on preventing intimal hyperplasia and restenosis. After hematoxylin eosin (HE) staining, typical cross-sections of arteries with implanted stents were showed in **Figure 7d**. Clearly, the co-grafted vascular stents could significantly reduce neo-intimal hyperplasia during the period of implantation as compared to the control. For example, after 12 weeks of implantation, the co-grafted stents showed remarkable decrease in mean neo-intimal stenosis ratio (**Figure 7e**, 34.4 % vs 20.4 %) and mean neo-intimal area (**Figure 7f**, 2.43 mm^2 vs 1.53 mm^2) as compared with the controls. Overall, the co-grafted vascular stents with optimized NO generation and EPC capture properties could significantly reduce ISR *in vivo*.

Discussion

Endothelium plays a key role in maintaining cardiovascular homeostasis. To prevent ISR after stenting, timely re-endothelialization onto the implanted stents is crucial. However, thrombogenic reaction, aggressive SMC proliferation, and sluggish EC migration at the interfaces of cardiovascular implants are all challenging in re-endothelialization. Over the past decades, surface conjugation of endothelium-specific motifs has been widely used to enhance endothelialization. A widely recognized consensus for vascular stent modification is that multifunctional coatings have superiority over the monofunctional ones for tackling the complicated pathological microenvironments. Unfortunately, multicomponent surface functionalization strategies generally suffer from complexity, poor controllability and low biocompatibility. Hence, we develop a biomimetic method for introducing a multicomponent, bioactive coating onto vascular stent surfaces by combining bio-orthogonal conjugation with mussel-inspired adhesive chemistry.

We select two endothelium-specific active moieties, the NO-generating SeCA and the EPC-binding TPS peptide, to optimize the vascular stents. This is because (1) NO is an endogenic signaling molecule capable of inhibition of platelets and SMCs, and (2) TPS peptide enables surface homing of circulating blood EPCs to accelerate endothelialization. The two vasoactive molecules thus include most of the cardiovascular functions of healthy endothelium. To improve biocompatibility, mussel-inspired peptide with clickable azido group ($(DOPA)_4$-PEG_5-Azide) was synthesized for the first-step grafting via mussel adhesion mechanism. By modifying SeCA and TPS peptide with DBCO, the two active moieties spontaneously bind onto the mussel-inspired peptide layer through bio-orthogonal click chemistry. Compared to traditional chemical means, the combination of mussel adhesion and bio-orthogonal chemistry feature simplicity, rapidness and high efficiency: the surface engineering procedure neatly sidesteps tedious reactions and sophisticated surface treatment technologies, reducing the damage towards the tethered bioactive molecules. Moreover, by controlling SeCA/TPS feeding ratio, the co-grafted surfaces exhibit tunable NO generation, thrombosis and SMC inhibition, excellent EPC capture, EC adhesion and proliferation, efficient re-endothelialization and prevention of ISR. We believe that our surface engineering strategy can be translated into new clinical coatings for cardiovascular stents and will benefit enormously and globally the cardiovascular disease patients; it will, furthermore, offer insights to engineering surfaces of blood-contacting devices.

Conclusion

In this work, we integrate multiple desirable functions into one metal vascular stent coating system through the mussel adhesive chemistry and bio-orthogonal conjugation. Our SeCA/TPS co-grafted coating is optimized with different SeCA/TPS feeding ratios and has achieved early anti-thrombosis, efficient SMC inhibition, potent EPC-capture capacity, rapid re-endothelialization and effective ISR prevention. In addition to the potential for addressing clinical complications of cardiovascular stents, this biomimetic surface bioengineering method also represents a promising strategy for controlling and optimizing multi-functionalization onto surfaces of other biomedical metallic materials.

Materials and Methods. Details of material synthesis, material characterization, cell culture, *in vitro*, *ex vivo* and *in vivo* tests are described in Supplementary Information (SI).

Data Availability Statement. All data for the paper are contained in the article and the SI.

Acknowledgements

The authors acknowledge the financial supports from the National Natural Science Foundation of China (31570957, 21875092, 91649204 and 21574091), the International Cooperation Project by Science and Technology Department of Sichuan Province (2019YFH0103), the Applied Basic Research Project funded by Sichuan Provincial Science and Technology Department (2017JY0296), the National Key Research and Development Program of China (2019YFA0112000), the Innovation and Entrepreneurship Program of Jiangsu Province, the "Six Talent Peaks" program of Jiangsu Province (2018-XCL-013), and the seed projects of Hong Kong Innovation and Technology Support Programme (ITS/065/19).

References

1. Sigwart U, Puel J, Mirkovitch V, Joffre F, Kappenberger L. Intravascular stents to prevent occlusion and re-stenosis after transluminal angioplasty. *New Engl. J. Med.* **316**, 701-706 (1987).
2. Roubin GS, *et al.* Intracoronary stenting for acute and threatened closure complicating percutaneous transluminal coronary angioplasty. *Circulation* **85**, 916-927 (1992).
3. Dangas GD, Claessen BE, Caixeta A, Sanidas EA, Mintz GS, Mehran R. In-stent restenosis in the drug-eluting stent era. *J. Am. Coll. Cardiol.* **56**, 1897-1907 (2010).
4. Lowe HC, Oesterle SN, Khachigian LM. Coronary in-stent restenosis: current status and future strategies. *J. Am. Coll. Cardiol.* **39**, 183-193 (2002).
5. Mehran R, *et al.* Angiographic patterns of in-stent restenosis: classification and implications for long-term outcome. *Circulation* **100**, 1872-1878 (1999).
6. De Scheerder I, *et al.* Experimental study of thrombogenicity and foreign body reaction induced by heparin-coated coronary stents. *Circulation* **95**, 1549-1553 (1997).
7. Tepe G, *et al.* Reduced thrombogenicity of nitinol stents—in vitro evaluation of different surface modifications and coatings. *Biomaterials* **27**, 643-650 (2006).
8. Kornowski R, Hong MK, Tio FO, Bramwell O, Wu H, Leon MB. In-stent restenosis: contributions of inflammatory responses and arterial injury to neointimal hyperplasia. *J. Am. Coll. Cardiol.* **31**, 224-230 (1998).
9. Mauri L, Hsieh W-h, Massaro JM, Ho KK, D'Agostino R, Cutlip DE. Stent thrombosis in randomized clinical trials of drug-eluting stents. *New Engl. J. Med.* **356**, 1020-1029 (2007).
10. Holmes DR, *et al.* Stent thrombosis. *J. Am. Coll. Cardiol.* **56**, 1357-1365 (2010).
11. Newby AC, Zaltsman AB. Molecular mechanisms in intimal hyperplasia. *J. Pathol.* **190**, 300-309 (2000).
12. Davies M, Hagen PO. Pathobiology of intimal hyperplasia. *Brit. J. Surg.* **81**, 1254-1269 (1994).
13. Puranik AS, Dawson ER, Peppas NA. Recent advances in drug eluting stents. *Int. J. Pharmaceut.* **441**, 665-679 (2013).

14. Shirota T, Yasui H, Shimokawa H, Matsuda T. Fabrication of endothelial progenitor cell (EPC)-seeded intravascular stent devices and in vitro endothelialization on hybrid vascular tissue. *Biomaterials* **24**, 2295-2302 (2003).
15. Avci-Adali M, Ziemer G, Wendel HP. Induction of EPC homing on biofunctionalized vascular grafts for rapid in vivo self-endothelialization — A review of current strategies. *Biotechnol. Adv.* **28**, 119-129 (2010).
16. Kong D, *et al.* Enhanced inhibition of neointimal hyperplasia by genetically engineered endothelial progenitor cells. *Circulation* **109**, 1769-1775 (2004).
17. Lan H, *et al.* Progress and prospects of endothelial progenitor cell therapy in coronary stent implantation. *J. Biomed. Mater. Res. B* **104**, 1237-1247 (2016).
18. de Mel A, Jell G, Stevens MM, Seifalian AM. Biofunctionalization of biomaterials for accelerated in situ endothelialization: a review. *Biomacromolecules* **9**, 2969-2979 (2008).
19. Li X, *et al.* Mussel-inspired "built-up" surface chemistry for combining nitric oxide catalytic and vascular cell selective properties. *Biomaterials* **241**, 119904 (2020).
20. Cui Y, *et al.* In situ endothelialization promoted by SEMA4D and CXCL12 for titanium-based biomaterials. In: *Seminars in thrombosis and hemostasis* (ed^(eds). Thieme Medical Publishers (2018).
21. Meyers SR, Hamilton PT, Walsh EB, Kenan DJ, Grinstaff MW. Endothelialization of titanium surfaces. *Adv. Mater.* **19**, 2492-2498 (2007).
22. Lin Q, Ding X, Qiu F, Song X, Fu G, Ji J. In situ endothelialization of intravascular stents coated with an anti-CD34 antibody functionalized heparin–collagen multilayer. *Biomaterials* **31**, 4017-4025 (2010).
23. Wang C-H, *et al.* Late-outgrowth endothelial cells attenuate intimal hyperplasia contributed by mesenchymal stem cells after vascular injury. *Arterioscl, Throm. Vas.* **28**, 54-60 (2008).
24. Zheng W, *et al.* Endothelialization and patency of RGD-functionalized vascular grafts in a rabbit carotid artery model. *Biomaterials* **33**, 2880-2891 (2012).
25. Zisch AH, Schenk U, Schense JC, Sakiyama-Elbert SE, Hubbell JA. Covalently conjugated VEGF–fibrin matrices for endothelialization. *J. Control. Release* **72**, 101-113 (2001).
26. Wissink M, *et al.* Improved endothelialization of vascular grafts by local release of growth factor from heparinized collagen matrices. *J. Control. Release* **64**, 103-114 (2000).
27. Ren X, *et al.* Surface modification and endothelialization of biomaterials as potential scaffolds for vascular tissue engineering applications. *Chem. Soc. Rev.* **44**, 5680-5742 (2015).
28. Li J, Zhang K, Huang N. Engineering cardiovascular implant surfaces to create a vascular endothelial growth microenvironment. *Biotechnol. J.* **12**, 1600401 (2017).
29. Lin Q, *et al.* Adhesion mechanisms of the mussel foot proteins mfp-1 and mfp-3. *P. Natl. Acad. Sci. USA* **104**, 3782-3786 (2007).
30. Lee H, Scherer NF, Messersmith PB. Single-molecule mechanics of mussel adhesion. *P. Natl. Acad. Sci. USA* **103**, 12999-13003 (2006).
31. Cha W, Meyerhoff ME. Catalytic generation of nitric oxide from S-nitrosothiols using immobilized organoselenium species. *Biomaterials* **28**, 19-27 (2007).

32. Veleva AN, Cooper SL, Patterson C. Selection and initial characterization of novel peptide ligands that bind specifically to human blood outgrowth endothelial cells. *Biotechnol. Bioeng.* **98**, 306-312 (2007).
33. Veleva AN, Heath DE, Cooper SL, Patterson C. Selective endothelial cell attachment to peptide-modified terpolymers. *Biomaterials* **29**, 3656-3661 (2008).
34. Patterson DM, Prescher JA. Orthogonal bioorthogonal chemistries. *Curr. Opin. Chem. Biol.* **28**, 141-149 (2015).
35. Ahanchi SS, Tsihlis ND, Kibbe MR. The role of nitric oxide in the pathophysiology of intimal hyperplasia. *J. Vasc. Surg.* **45**, A64-A73 (2007).
36. Naghavi N, de Mel A, Alavijeh OS, Cousins BG, Seifalian AM. Nitric Oxide Donors for Cardiovascular Implant Applications. *Small* **9**, 22-35 (2013).
37. Elnaggar MA, *et al.* Nitric Oxide Releasing Coronary Stent: A New Approach Using Layer-by-Layer Coating and Liposomal Encapsulation. *Small* **12**, 6012-6023 (2016).
38. Pan G, *et al.* Biomimetic Design of Mussel-Derived Bioactive Peptides for Dual-Functionalization of Titanium-Based Biomaterials. *J. Am. Chem. Soc.* **138**, 15078-15086 (2016).
39. Ma Y, He P, Tian X, Liu G, Zeng X, Pan G. Mussel-Derived, Cancer-Targeting Peptide as pH-Sensitive Prodrug Nanocarrier. *ACS Appl. Mater. Inter.* **11**, 23948-23956 (2019).
40. Liu L, Tian X, Ma Y, Duan Y, Zhao X, Pan G. A Versatile Dynamic Mussel-Inspired Biointerface: From Specific Cell Behavior Modulation to Selective Cell Isolation. *Angew. Chem. Int. Ed.* **57**, 7878-7882 (2018).
41. Das TK, Ganguly S, Ghosh S, Remanan S, Ghosh SK, Das NC. In-situ synthesis of magnetic nanoparticle immobilized heterogeneous catalyst through mussel mimetic approach for the efficient removal of water pollutants. *Colloid and Interface Science Communications* **33**, 100218 (2019).
42. Yang Z, Yang Y, Xiong K, Wang J, Lee H, Huang N. Metal-phenolic surfaces for generating therapeutic nitric oxide gas. *Chem. Mater.* **30**, 5220-5226 (2018).
43. Li J, De Rosa S, Wang J, Zhang K. Biomaterials Development, Modification, and Potential Application for Interventional Cardiology. *BioMed Research International* **2020**, 4890483 (2020).
44. Xu X, Wang L, Wang G, Jin Y. The effect of REDV/TiO2 coating coronary stents on in-stent restenosis and re-endothelialization. *Journal of biomaterials applications* **31**, 911-922 (2017).
45. Zhang F, Zhang Q, Li X, Huang N, Zhao X, Yang Z. Mussel-inspired dopamine-CuII coatings for sustained in situ generation of nitric oxide for prevention of stent thrombosis and restenosis. *Biomaterials* **194**, 117-129 (2019).
46. He JZ, Ho JD, Gingerich S, Courtman DW, Marsden PA, Ward ME. Enhanced translation of heme oxygenase-2 preserves human endothelial cell viability during hypoxia. *J. Biol. Chem.* **285**, 9452-9461 (2010).
47. Martin E, Berka V, Tsai AL, Murad F. Soluble guanylyl cyclase: the nitric oxide receptor. *Method. Enzymol.* **396**, 478-492 (2005).
48. Qiu H, *et al.* Biomimetic engineering endothelium-like coating on cardiovascular stent through heparin and nitric oxide-generating compound synergistic modification strategy. *Biomaterials* **207**, 10-22 (2019).

49. Yang Y, *et al.* Endothelium-Mimicking Multifunctional Coating Modified Cardiovascular Stents via a Stepwise Metal-Catechol-(Amine) Surface Engineering Strategy. *Research* **2020**, 20 (2020).
50. Seo H-R, *et al.* Intrinsic FGF2 and FGF5 promotes angiogenesis of human aortic endothelial cells in 3D microfluidic angiogenesis system. *Sci. Rep.* **6**, 28832 (2016).
51. Wei Y, *et al.* Surface engineering of cardiovascular stent with endothelial cell selectivity for in vivo re-endothelialisation. *Biomaterials* **34**, 2588-2599 (2013).
52. Medina-Leyte DJ, Domínguez-Pérez M, Mercado I, Villarreal-Molina MT, Jacobo-Albavera L. Use of Human Umbilical Vein Endothelial Cells (HUVEC) as a Model to Study Cardiovascular Disease: A Review. *Applied Sciences* **10**, 938 (2020).
53. Cornwell TL, Arnold E, Boerth NJ, Lincoln TM. Inhibition of smooth muscle cell growth by nitric oxide and activation of cAMP-dependent protein kinase by cGMP. *American Journal of Physiology-Cell Physiology* **267**, C1405-C1413 (1994).
54. Lertkiatmongkol P, Liao D, Mei H, Hu Y, Newman PJ. Endothelial functions of PECAM-1 (CD31). *Curr. Opin. Hematol.* **23**, 253 (2016).